

RESEARCH ARTICLE

Open Access

The dynamical study of O(¹D) + HCl(v = 0, j = 0) reaction at hyperthermal collision energies

Meihua Ge*, Huan Yang and Yujun Zheng

Abstract

Backgrounds: The quasi-classical trajectory calculations for O(¹D) + HCl → OH + Cl (R1) and O(¹D) + HCl → ClO + H (R2) reactions have been performed at hyperthermal collision energies (60.0, 90.0, and 120.0 kcal/mol) on the ¹A' state. Reaction probabilities and integral cross sections are calculated. The product rotational distributions for the two channels, and the product rotational alignment parameters are investigated. Also, the alignment and the orientation of the products have been predicted through the angular distribution functions (concerning the initial/final velocity vector, and the product rotational angular momentum vector). To have a deeper understanding of the natures of the vector correlation between reagent and product relative velocities, a natural generalization of the differential cross section PPDCS_{000} is calculated.

Results: The OH + Cl channel is the main product channel and is observed to have essentially isotropic rotational distributions. The ClO + H channel is found to be clearly rotationally polarized.

Conclusions: The dynamical, especially the stereodynamical characters are quite different for the two channels of the title reaction. Most reactions occur directly, except for R2 reaction at the collision energies of 60.0 and 120.0 kcal/mol. The alignment and orientation effects are weak/strong for R1/R2 reaction. The well structure on the potential energy surface and hyperthermal collision energies might result in the dynamical effects.

Keywords: O(¹D) + HCl, Hyperthermal, Stereodynamics, Alignment, Orientation

Background

Considerable attention has been devoted to the O(¹D) + HCl reaction [1-22], due in part, to its significant role in stratospheric chemistry. Using *ab initio* self-consistent field (SCF) and configuration interaction (CI) methods, Bruna *et al.* [1] reported potential curves for the ground and various valence and Rydberg excited states of HOCl and HClO. The angular and velocity distributions of ClO product from the reaction of O(¹D) + HCl at 12.2 kcal/mol collision energy were calculated in a crossed-molecular-beam study in Ref. [2]. Experimentally, the reactions of O(¹D) + HCl → OH + Cl and OCl + H were studied at an average collision energy of 7.6, 7.7, and 8.8 kcal/mol through the resonance-enhanced multiphoton ionization technique [3]. Nascent state-resolved ClO ($X^2\Pi$) radicals produced in reaction of O(¹D) with HCl were measured

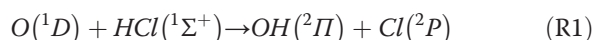
by employing the technique of vacuum-ultraviolet laser-induced fluorescence [4]. Hernandez *et al.* [5] calculated the potential energy surface (PES) of the O(¹D) + HCl reaction and performed a quasi-classical trajectory (QCT) study on this PES. Cross sections over the collision energy range of 0.0-20.0 kcal/mol were presented and product angular distributions were given at the collision energies of 7.6 and 12.2 kcal/mol. Alvariño *et al.* [6] studied the dependence of calculated product rotational polarization on the scattering angle for the title reaction using QCT method. An accurate *ab initio* HOCl PES was constructed by Skokov *et al.* [7] in 1998. Through a QCT calculation [8], the product angular distribution and dihedral angle distribution for the ClO forming process are performed together with product vibrational distribution for the OH forming process. The quantum and QCT reaction probabilities (RPs) [9] were presented over the collision energy range of 2.3-18.4 kcal/mol by Christoffel *et al.*. At the collision energy of 12.2 kcal/mol, integral cross sections (ICSs) for vibrational states summed over rotational states for the ClO and OH products, and translational energy

* Correspondence: mhge@sdu.edu.cn
School of Physics, Shandong University, Jinan 250100, China

distributions of the ClO product were also performed [9]. Based on Ref. [7], a global PES was constructed for the X¹A' electronic ground state of HOCl including the accurate HClO isomer [10]. Vibrational energy levels and intensities were computed for both HOCl and HClO up to the OH + Cl dissociation limit and above the isomerization barrier using the PES of Ref. [10]. Bittererová *et al.* [11] performed a wave-packet calculation to study the effect of reactant rotation and alignment on product branching in the O(¹D) + HCl → ClO + H, OH + Cl reactions using the PES of Ref. [10]. A new fit to extensive *ab initio* calculations of a global potential [10] and the quantum wave packet calculations of the O(¹D) + HCl → ClO + H, OH + Cl reactions were reported by Bittererová *et al.* [12]. Accurate time-dependent wavepacket calculation for the O(¹D) + HCl reaction was carried out by Lin *et al.* [13]. Recently, we have studied the effects of the collision energy and reagent vibrational excitation on the reaction of O(¹D) + HCl → OH + Cl [22].

However, most of these studies were focused on the case of low collision energies. As well known, hyperthermal collisions act a part in the chemistry of extreme environments, such as those encountered in plasma, rocket plumes, and space vehicles in low-earth orbit. The hyperthermal O + HCl chemistry plays an important role in the reacting flows coming from the interaction of a jet and the rarefied atmosphere [23], and we need the data of accurate reaction cross sections and branching ratios at high collision energies to assess its importance. The dynamics of high-energy collisions remains mostly unexplored, and there are only a few studies concerned with the O(³P) + HCl reaction [24,25].

The title reaction is especially demanding, and interesting, due to the presence of two product channels,



As noted in Ref. [12], when the collision energy is below 0.55 eV (12.68 kcal/mol), the quantum integral cross sections (ICSs) display an inverse dependence on the collision energy, and the OH product is favoured over the ClO product. But what will happen when the collision energy is hyperthermal?

In this paper, based on the recent-developed ¹A' PES [12], a quasi-classical trajectory (QCT) calculation is performed on the O(¹D) + HCl(v = 0, j = 0) reaction so as to study the dynamical, especially the stereodynamical characteristics at hyperthermal collision energies. To evaluate the importance of the hyperthermal O + HCl chemistry, RPs, cross sections

and branching ratios at high collision energies are investigated. Also, our investigation can provide necessary data to the hyperthermal O + HCl chemistry. The products for R1 and R2 reactions have hot rotational populations. Alignment and orientation effects are shown through two angular distribution functions. The scattering directions of the products are also studied through the PDDCS₀₀ results. The statistical errors are marked as error bars in the Figures.

Methodology and computational details

In the framework of quasi-classical trajectory (QCT) approach [21,22,26–34], the center-of-mass (CM) frame is used. The reagent relative velocity vector \mathbf{k} is chosen to be parallel to the z axis, and the scattering plane contains the initial and final velocity vectors (noted as \mathbf{k} and \mathbf{k}' , respectively). In the CM frame, θ_r and ϕ_r are the corresponding polar and azimuthal angles of the product rotational momentum \mathbf{j}' , respectively. The scattering angle between \mathbf{k} and \mathbf{k}' is marked as θ_t , namely

$$\cos\theta_t = \frac{(\mathbf{k} \cdot \mathbf{k}')}{(|\mathbf{k}| \cdot |\mathbf{k}'|)}. \quad (1)$$

The numbers of reactive trajectory and total trajectory are marked as N_r and N_{tot} in due order. The RP can be expressed as

$$P = \frac{N_r}{N_{tot}}. \quad (2)$$

The ICS σ can be defined as

$$\sigma = \pi b_{max}^2 \frac{N_r}{N_{tot}}, \quad (3)$$

where b_{max} denotes the maximum value of the impact parameter b .

The associated uncertainties with the ICS can be calculated according to $\Delta\sigma = [(N_{tot} - N_r)/(N_{tot} \cdot N_r)]^{1/2}\sigma$.

The differential cross section (DCS) is given by

$$\frac{d\sigma}{d(\cos\theta_t)} = \frac{N_r(\theta_t) \cdot \pi b_{max}^2}{2\pi \sin\theta_t \cdot N_{tot}}. \quad (4)$$

During reactive encounter, the total angular momentum is conserved [26]

$$\mathbf{j} + \mathbf{l} = \mathbf{j}' + \mathbf{l}', \quad (5)$$

here \mathbf{l} and \mathbf{l}' are the reagent and product orbital momenta, respectively. When j is small (as is common), the rotation of the product can only result from \mathbf{l} . The distribution of \mathbf{j}' is described by $P(\theta_r)$, which can be expanded by a set of Legendre polynomials

$$P(\theta_r) = \frac{1}{2} \sum (2k+1) a_0(k) P_k(\cos\theta_r). \quad (6)$$

Here the polarization parameter $a_0(k)$ can be expressed as

$$a_0(k) = \int_0^\pi P(\theta_r) P_k(\cos\theta_r) \sin\theta_r d\theta_r = \langle P_k(\cos\theta_r) \rangle. \quad (7)$$

$a_0(2)$ indicates the product rotational alignment

$$a_0(2) = \langle P_2(\cos\theta_r) \rangle = \frac{1}{2} \langle 3\cos^2\theta_r - 1 \rangle. \quad (8)$$

$P(\phi_r)$ denotes the dihedral angle distribution, which can be expanded in the Fourier series

$$P(\phi_r) = \frac{1}{2\pi} \left[1 + \sum_{even, n \geq 2} a_n \cos(n\phi_r) + \sum_{odd, n \geq 1} b_n \sin(n\phi_r) \right]. \quad (9)$$

The expansion coefficients a_n and b_n are given by

$$a_n = 2 \langle \cos n\phi_r \rangle, \quad (10)$$

$$b_n = 2 \langle \sin n\phi_r \rangle. \quad (11)$$

The full three-dimensional angular distribution associated with $\mathbf{k}\cdot\mathbf{k}'\cdot\mathbf{j}'$ correlation can be expressed as

$$P(\omega_t, \omega_r) = \sum_{kq} \frac{2k+1}{4\pi} \frac{1}{\sigma} \frac{d\sigma_{kq}}{d\omega_t} C_{kq}(\theta_r, \phi_r)^*, \quad (12)$$

where $C_{kq}(\theta_r, \phi_r)$ are the modified spherical harmonics and the angles $\omega_t = \theta_t, \phi_t$ and $\omega_r = \theta_r, \phi_r$ refer to the coordinates of the unit vectors \mathbf{k}' and \mathbf{j}' along the directions of the product relative velocity and rotational angular momentum vectors, respectively. $\frac{1}{\sigma} \frac{d\sigma_{kq}}{d\omega_t}$ is a generalized polarization-dependent differential cross section (PDDCS), and it can be written as

$$\frac{1}{\sigma} \frac{d\sigma_{kq}}{d\omega_t} = \sum_{kq} \frac{2k+1}{4\pi} S_{kq}^{k_1} C_{k_1 q}(\theta_t, 0). \quad (13)$$

Here the expectation value $S_{kq}^{k_1}$ is given by

$$S_{kq}^{k_1} = \langle C_{k_1 q}(\theta_t, 0) C_{kq}(\theta_r, 0) [(-1)^q e^{iq\Phi_r} \pm e^{-iq\Phi_r}] \rangle. \quad (14)$$

The angular brackets $\langle \dots \rangle$ in Eq. (14) represent the average over all angles.

The initial ro-vibrational quantum numbers of the HCl reactant are set as $v=0$, and $j=0$. 1,000,000 trajectories are used on the ${}^1A'$ electronic states at the collision energies of 60.0, 90.0 and 120.0 kcal/mol. The time integral step size is 10^{-4} ps. The maximum values of impact parameter b_{\max} are 2.80/1.15 (60.0 kcal/mol), 2.81/1.55 (90.0 kcal/mol), and 2.86/1.05 (120.0 kcal/mol) for R1/R2 reaction and the unit is in Angstrom.

The PES we used is constructed by Bittererová *et al.* [12]. The title reaction proceeds without a barrier to either set of products, but via two complex regions, HOCl and HClO. For R1 (R2) reaction, according to Ref. [12], ${}^1A'$ state has a deep well in bent geometry corresponding to stable HOCl (HClO) molecule and the well depth is -102.16 (-48.20) kcal/mol. The schematic of the energetics of the $O({}^1D) + HCl$ *ab initio* global potential is exhibited in Figure 1.

For the $A + BC \rightarrow AB + C$ reaction, in the impulse model [27], the product rotational angular momentum \mathbf{j}' could be described with the reagent orbital and rotational angular momenta, \mathbf{l} and \mathbf{j} , i.e. $\mathbf{j}' = \mathbf{l} \sin^2\beta + \mathbf{j} \cos^2\beta + \mathbf{J}_1 \frac{m_B}{m_{AB}}$, where $\mathbf{J}_1 = \sqrt{\mu_{BC} R} (\mathbf{r}_{AB} \times \mathbf{r}_{CB})$ and $\cos^2\beta = \frac{m_A m_C}{(m_A + m_B)(m_B + m_C)}$. μ_{BC} is the reduced mass of the BC molecule, R , the repulsive energy, and $\mathbf{r}_{AB}, \mathbf{r}_{CB}$, the unit vectors where B points to A and where B points to C, respectively, β is known as the skew angle. For R1 (R2) reaction, $\beta \approx 17^\circ$ ($\beta \approx 85^\circ$), which is a pretty small (large) angle. Larger polarization properties are expected for the products with the smaller value of $\cos^2\beta$ (i.e. R2 reaction) according to the kinematic limit, which could be observed via the alignment parameters. \mathbf{l}

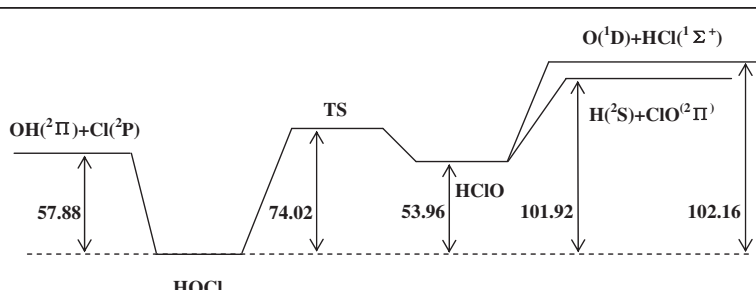


Figure 1 The schematic of the energetics (in kcal/mol) of the $O({}^1D) + HCl$ *ab initio* global potential.

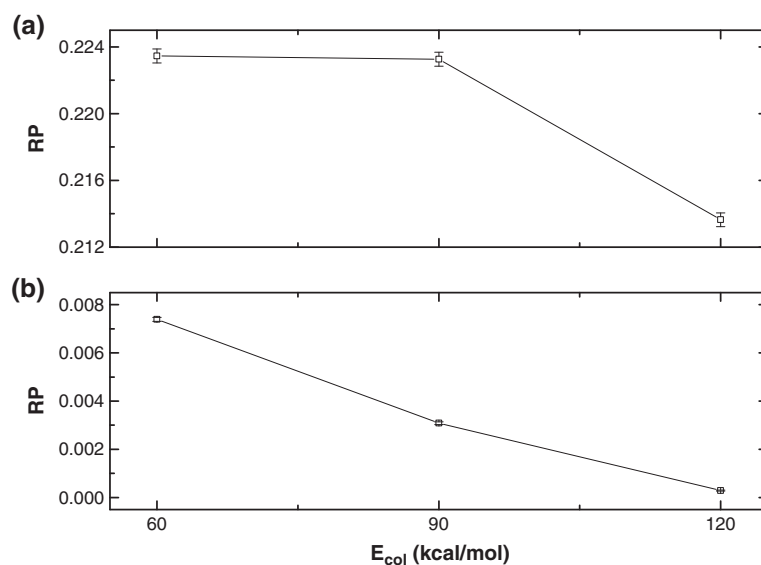


Figure 2 RPs at the collision energies of 60.0, 90.0 and 120.0 kcal/mol for (a) $\text{O} + \text{HCl} \rightarrow \text{OH} + \text{Cl}$ (R1), and (b) $\text{O} + \text{HCl} \rightarrow \text{ClO} + \text{H}$ (R2) reactions.

$\sin^2\beta + j \cos^2\beta$ is symmetric, which leads to the symmetric distribution of $P(\theta_r)$ in Figure 2. However, $\frac{J_{1MB}}{m_{AB}}$ shows a preferred direction due to the repulsive energy and results in the biased orientation of the products as shown in $P(\phi_r)$ distributions.

Results and discussion

The results for R1 and R2 reactions are found to be quite different due to the different dynamical reaction channels, which can also be observed in the

two (HF and DF) product channels of $\text{F} + \text{HD}$ reaction [35].

RPs and ICSs

Figures 2 and 3 show the results of RPs and ICSs at the collision energies of 60.0, 90.0, and 120.0 kcal/mol. The OH products shown in Figure 2(a) and Figure 3(a) are apparently favoured over the ClO products shown in Figure 2(b) and Figure 3(b), which agrees well with the quantum results at low collision energies [12]. With the increase of the

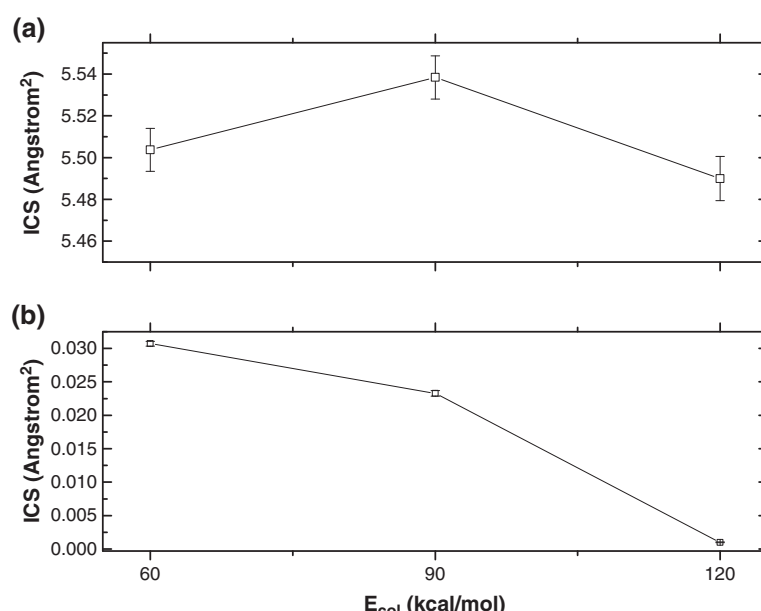


Figure 3 ICSs at the collision energies of 60.0, 90.0 and 120.0 kcal/mol for (a) $\text{O} + \text{HCl} \rightarrow \text{OH} + \text{Cl}$ (R1), and (b) $\text{O} + \text{HCl} \rightarrow \text{ClO} + \text{H}$ (R2) reactions.

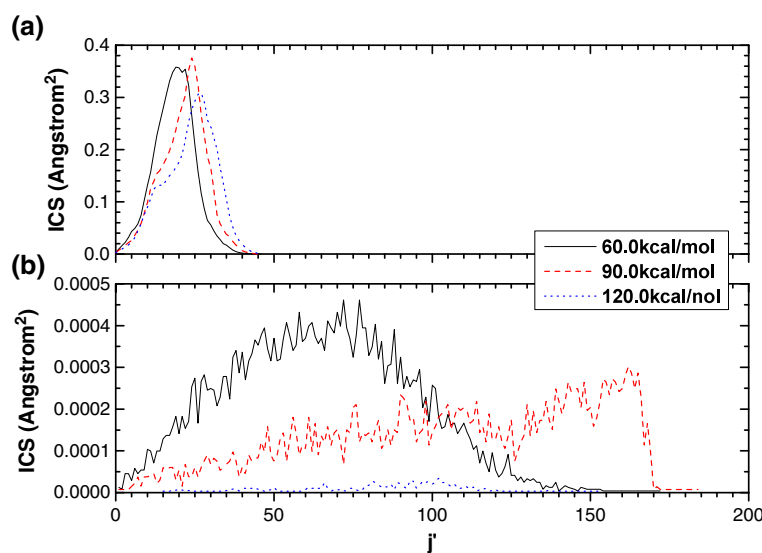


Figure 4 PRDs for (a) $O + HCl \rightarrow OH + Cl$ (R1), and (b) $O + HCl \rightarrow ClO + H$ (R2) reactions.

collision energy, both RP and ICS obviously decrease except for ICS at the collision energy of 90.0 kcal/mol for R1 reaction. The title reaction proceeds without a potential barrier and typically by complex formation, which can be displayed through the quantum RPs [12]. This oscillating structure might cause the translational excitation to impede the reaction. Also, the quantum ICSs [12] show the inverse

dependence on the initial relative kinetic energy, and the OH product is favoured over the ClO product. The statistical errors for RPs are $\pm 0.00042 / \pm 0.000086$, $\pm 0.00042 / \pm 0.000055$, $\pm 0.00041 / \pm 0.000017$ for R1/R2 reaction at $E_{col} = 60.0$, 90.0 and 120.0 kcal/mol, respectively.

The branching ratios $\frac{\sigma_{ClO}}{\sigma_{OH}}$ are about $0.0056 (\pm 0.000075)$, $0.0042 (\pm 0.000084)$ and $0.0002 (\pm 0.000011)$ at the

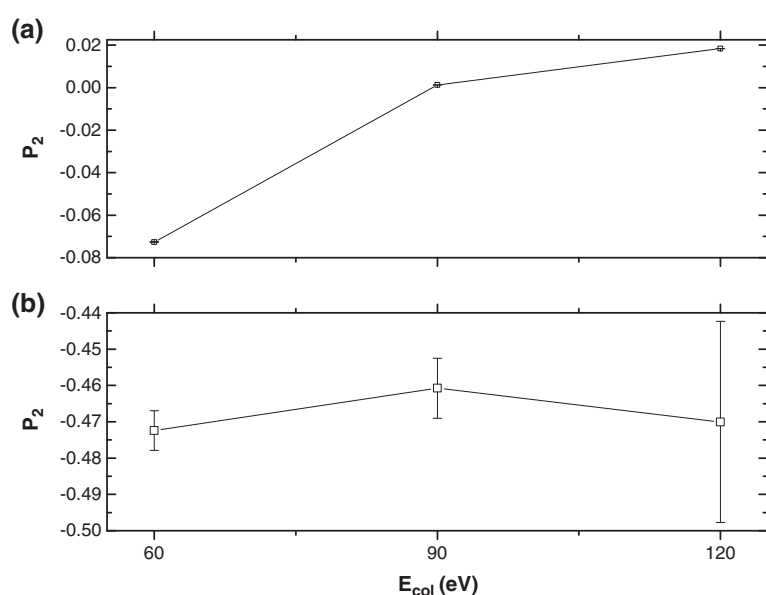


Figure 5 P_2 values at the collision energies of 60.0, 90.0 and 120.0 kcal/mol for (a) $O + HCl \rightarrow OH + Cl$ (R1), and (b) $O + HCl \rightarrow ClO + H$ (R2) reactions.

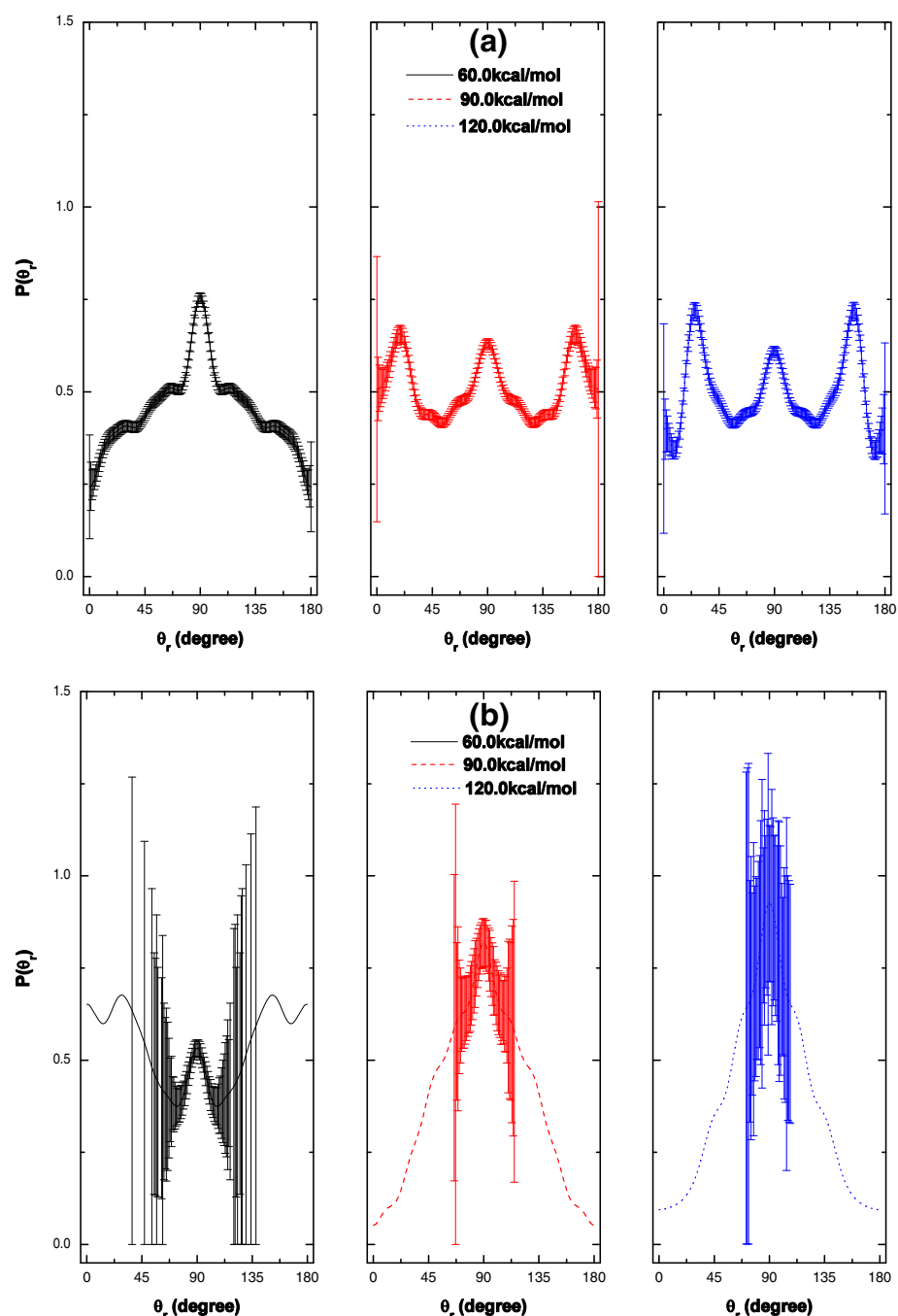


Figure 6 $P(\varphi_r)$ distributions at the collision energies of 60.0, 90.0 and 120.0 kcal/mol for (a) $O + HCl \rightarrow OH + Cl$ (R1), and (b) $O + HCl \rightarrow ClO + H$ (R2) reactions.

collision energies of 60.0, 90.0 and 120.0 kcal/mol in due order. It is obvious that the branching ratio rapidly decreases with the increase in the collision energy. The branching ratios are much smaller than those at the lower collision energies [2,3,12,14].

The product rotational distributions (PRDs)

Figure 4 shows the PRDs of R1 (as shown in Panel (a)) and R2 (as shown in Panel (b)) reactions. Obviously, the products for R1 and R2 reactions are rotationally hot. The peak shifts towards larger rotational quantum numbers except for R2 reaction at the collision energy of

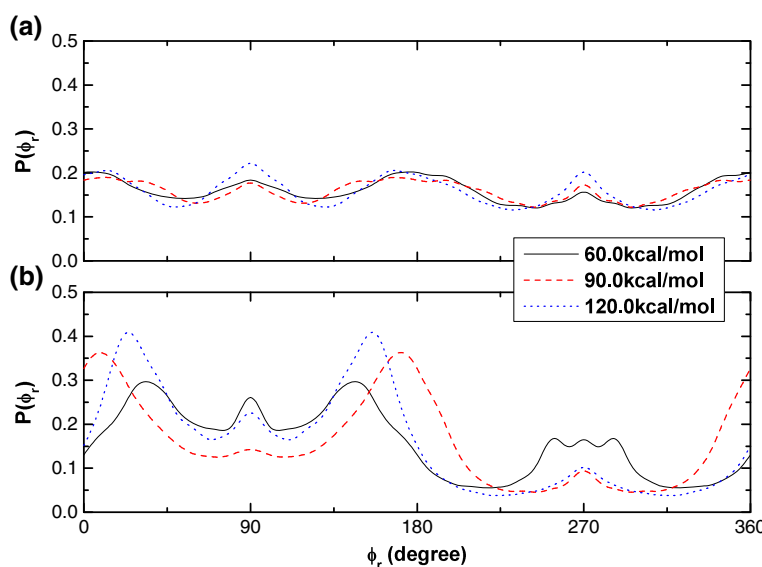


Figure 7 $P(\theta_r)$ Distributions at the collision energies of 60.0, 90.0 and 120.0 kcal/mol for (a) $O + HCl \rightarrow OH + Cl$ (R1), and (b) $O + HCl \rightarrow ClO + H$ (R2) reactions.

120.0 kcal/mol. The PRDs of R2 reaction show much broader ranges than those of R1 reaction due to larger polarization properties for R2 as mentioned above. For the $Li + HF \rightarrow Li + F$ reaction (which also belongs to Heavy heavy-Light (HHL) scheme), LiF product is also produced in highly excited states [35,36].

As mentioned in Refs. [35-37], vector correlation of angular momentum orientation and alignment in chemical reactions can provide rich information on the reaction dynamics. By analyzing the alignment parameters, two angular distributions ($P(\theta_r)$ and $P(\phi_r)$), and PDDCS₀₀, we can get a view of the stereodynamical information of the title reaction.

The product rotational alignment

For R1 reaction as shown in Figure 5(a), P_2 slightly increases with the increase of the collision energy. The value of P_2 becomes less negative (-0.073, 0.001, and 0.018 for $E_{col} = 60.0, 90.0$ and 120.0 kcal/mol, respectively) and the product rotational angular momentum tends to have a less anisotropic distribution. With the increase of the collision energy, the degree of alignment is almost invariant (only slightly increases) which could be ascribed to the Heavy Light-heavy (HLH) mass combination [6]: much angular momentum transfers from the reagent orbit to the product orbit, $\mathbf{l-l'}$, and little to rotation. Therefore, large variations in the direction of $\mathbf{j'}$ are needed for compensating even small variations in $\mathbf{l'}$.

For R2 reaction, the P_2 values at the three collision energies are approaching to -0.5, which indicates that the

product rotation strongly aligned perpendicular to the reagents' relative velocity \mathbf{k} . This is a typical feature of the HHL system [6,26,35,36]. A significant feature of this kind of reaction is the kinematic limit, *i.e.*, the initial orbital angular momentum \mathbf{l} completely goes into the product rotational angular momentum $\mathbf{j'}$, which leads to the alignment character. This is consistent with the alignment of $Li + HF \rightarrow LiF + H$ [35,36]. The significant disposal of angular momentum in the product orbital motion, $\mathbf{l} \rightarrow \mathbf{j}' + \mathbf{l}'$ declines the product rotational alignment, particularly at lower collision energies, so the calculated P_2 values deviate slightly from -0.5, which could also be supported by the $P(\theta_r)$ results.

According to the results of $H^+ + D_2(v=0, j=0) \rightarrow HD(v', j') + D^+$ reaction [37], the alignment of rotational angular momentum of HD products is nearly always close to zero due to the long-lived resonances. However, $H^+ + D_2(v=0, j=0) \rightarrow HD(v', j') + D^+$ reaction belongs to Light light-light (LLL) scheme, and in the reference [37] the alignment is state-resolved, however, our results are the sum of all states. So there are different results for the alignment parameters. And through the observation of three internuclear distances with the propagation of collision time, we can find that the reactions proceed directly except for the collision energies of 60.0 and 120.0 kcal/mol for R2 reaction.

$P(\theta_r)$ distributions

$P(\theta_r)$ is the distribution function reflecting the $\mathbf{k-j'}$ correlation, which is sensitive to two factors: the characters

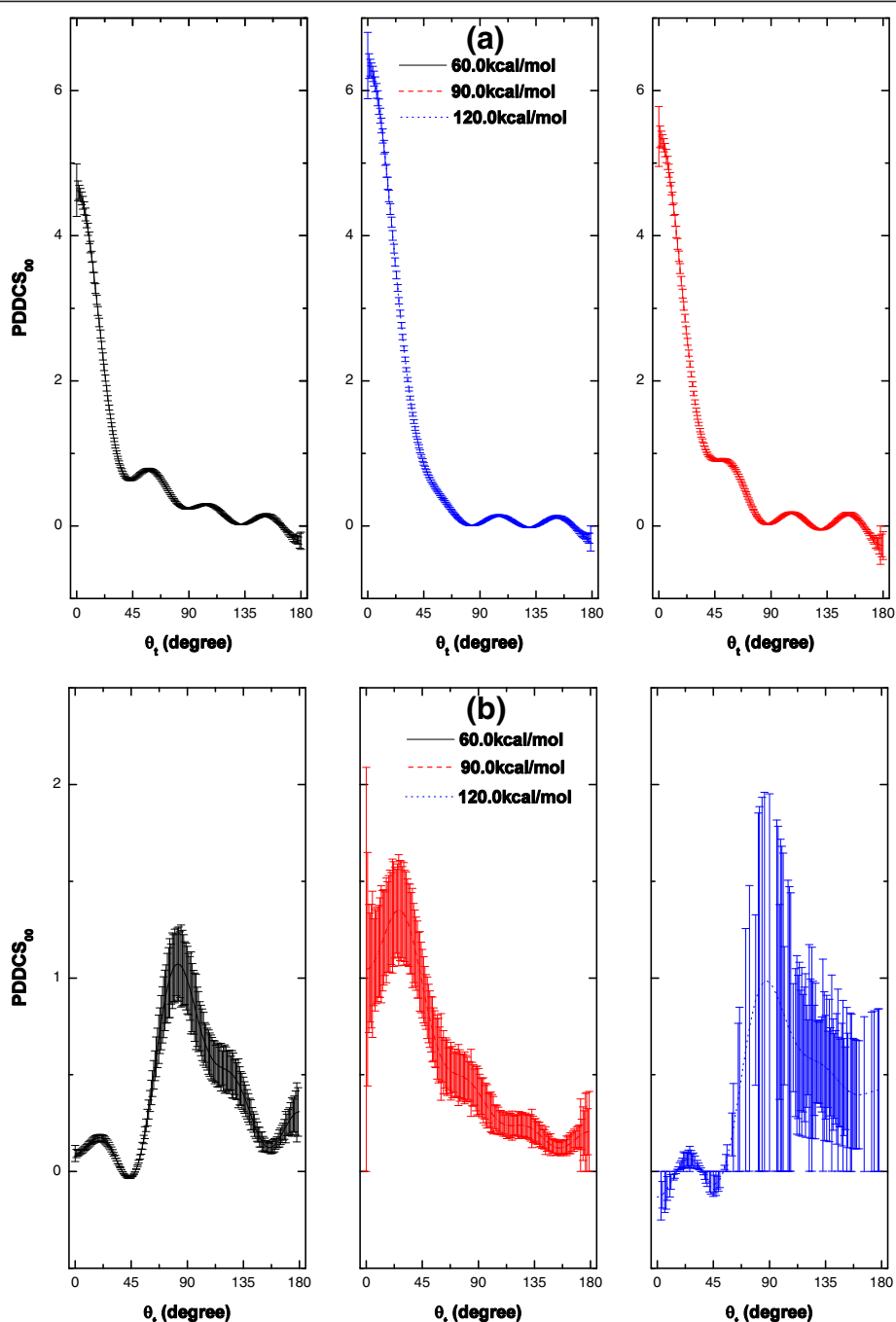


Figure 8 $PDDCS_{00}$ as a function of scattering angle at the collision energies of 60.0, 90.0 and 120.0 kcal/mol for (a) $O + HCl \rightarrow OH + Cl$ (R1), and (b) $O + HCl \rightarrow ClO + H$ (R2) reactions.

of PES and the mass factor. Obviously, there is a discrepancy between $P(\theta_r)$ distributions of the two reactions due to the different mass factors of the two reactions. For R1 and R2 reactions, at all the collision energies, the $P(\theta_r)$ distribution functions are symmetric with respect to $\theta_r = 90^\circ$ as analyzed above. The alignment effects are

obscure /obvious for R1/R2 reaction, which is supported by $P(\phi_r)$ distributions in Figure 7.

For R1 reaction shown in Panel (a), the largest peak appears at $\theta_r = 90^\circ$ at $E_{col} = 60.0$ kcal/mol. At the collision energy of 90.0 kcal/mol, the largest peaks are around $\theta_r = 90^\circ$, 20° and 160° . Around $\theta_r = 26^\circ$ and 154° , there are the largest two peaks at $E_{col} = 120.0$ kcal/mol.

For R2 reaction shown in Panel (b), it is a HHL system, with the mass factor – $\cos^2\beta = \frac{m_O m_H}{(m_O + m_{Cl})(m_{Cl} + m_H)} \approx 0.0086$ approaching to zero, which manifests that the product rotational alignment is strong with regard to the initial velocity vector \mathbf{k} [26], which could be also

observed through the alignment parameter in Figure 5 (b) and $P(\phi_r)$ distributions in Figure 7(b).

$P(\phi_r)$ distributions

$P(\phi_r)$ describes the $\mathbf{k}\cdot\mathbf{k}'\cdot\mathbf{j}'$ correlation, which reflects the polarization of product rotational angular momentum j' . The $P(\phi_r)$ distribution is asymmetric with respect to the

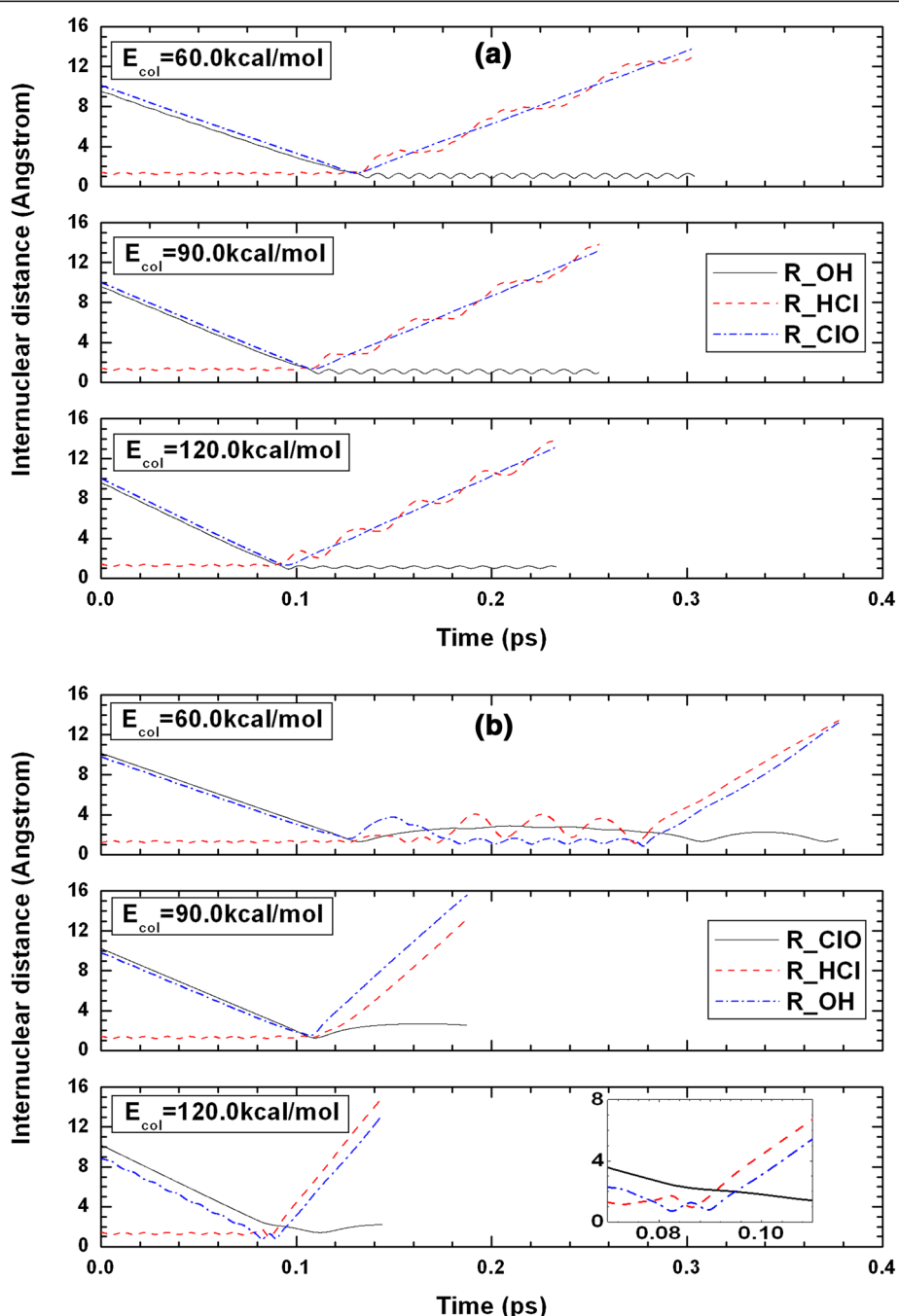


Figure 9 Internuclear distances of OH, HCl and ClO (marked as R_OH, R_HCl and R_CIO, respectively) as a function of propagation time at 60.0, 90.0 and 120.0 kcal/mol for (a) O + HCl → OH + Cl (R1), and (b) O + HCl → ClO + H (R2) reactions.

$\mathbf{k}\mathbf{k}'$ scattering plane (*i.e.* at about $\phi_r = 180^\circ$), which could be explained by the impulse model [27] as mentioned above.

For R1 reaction in Figure 7(a), there are only several small peaks, implying that the orientation effects are not obvious at the three different collision energies, which agrees well with the alignment parameter in Figure 5(a) and $P(\theta_r)$ distributions in Figure 6(a).

For R2 reaction in Figure 7(b), the largest peaks appear around $\phi_r = 0^\circ$ (or 360°)/ $\phi_r = 180^\circ$, implying that the ClO molecular axis vector orients along $x/-x$ axis.

PDDCS₀₀

PDDCS₀₀ is proportional to DCS, which can be used to describe the $\mathbf{k}\mathbf{k}'$ correlation. Through PDDCS₀₀, we can study the scattering direction of the product.

For OH + Cl products (R1 reaction), obvious forward scattering is exhibited in Figure 8(a). The distribution is asymmetric with respect to $\theta_t = 90^\circ$, and the peaks are found around $\theta_t = 0^\circ$, which indicates that the impact time is short and that direct reaction dominates. Usually, the deep well results in a long-lived reaction intermediate. However, according to the PDDCS₀₀ results, direct reaction dominates at high collision energies. The internuclear distances of OH, HCl and ClO (labeled as R_OH, R_HCl, and R_ClO, respectively) as a function of propagation time are shown in Figure 9(a), which gives a proof of the direct reaction. For R1 reaction, the reaction times are short at the three collision energies.

For ClO + H products (R2 reaction), as shown in Figure 8(b), the distribution is observed to be almost backward-forward symmetric with backward scattering being slightly favoured, except for the case of $E_{\text{col}} = 90.0$ kcal/mol. We can deduce that part of the reaction occurs via a long-lived complex and part via direct abstraction of Cl atom, which is also a remarkable conclusion of Ref. [2,5]. Moreover, the peaks locate close to $\theta_t = 90^\circ$. H atom (with very slight mass) is one of the products, so the reduced mass of the products is also very small, which causes the products orbital angular momentum I' to be smaller than the products rotational angular momentum j' and the final relative velocity vector \mathbf{k}' no longer to be remained in the xz plane. Of course, the scattering of the products is still cylindrically symmetric around z axis (\mathbf{k}). So, the separation of H atom and ClO molecule is almost along the direction that perpendicular to the incoming direction of O atom (*i.e.* the direction of \mathbf{k}). This results in the dominant population of the products along $\theta_t = 90^\circ$. In Figure 9(b), the oscillating structures at the collision energies of 60.0 and 120.0 kcal/mol show that the complexes have long lifetimes compared with the reaction period. Also obviously, the direct reaction occurs at the collision energy of 90.0 kcal/mol.

Conclusions

For the title reaction, the dynamics of the two product channels through a QCT calculation have been investigated. The RPs, cross sections and branching ratios at high collision energies have been presented and it is found that branching ratio rapidly decreases with the increase of the collision energy. The products are rotationally hot for both R1 and R2 reactions. The alignment and the orientation of the products have been studied, together with the scattering distributions. The HLH channel— OH + Cl (R1 reaction) is the main one as described before. R1 is observed to have essentially isotropic rotational distributions. On the contrary, the HHL one— ClO + H (R2 reaction) is found to be clearly rotationally polarized. The phenomena are probably due to the well structure of the PES and the hyperthermal collision energies. Through PDDCS₀₀ results of the O + HCl channel, it is obvious that the impact time is short and that direct reaction dominates. We attribute this to the hyperthermal collisions. However, indirect reactions dominate for the ClO + H channel at the collision energies of 60.0 and 120.0 kcal/mol.

Competing interests

Are there any non-financial competing interests (political, personal, religious, ideological, academic, intellectual, commercial or any other) to declare in relation to this manuscript? The authors declare that they have no competing interests.

Authors' contributions

MG carried out the calculation and drafted the manuscript. MG, HY and YZ analyzed the results. MG, HY and YZ corrected the English expressions. All authors have read and approved the final manuscript.

Acknowledgements

The work was supported by the National Natural Science Foundation of China (Grant Nos. 21073110, 11204159 and 21203108), and Natural Science Foundation of Shandong Province, China (Grand No. ZR2012AQ002).

Received: 17 March 2013 Accepted: 7 November 2013

Published: 15 November 2013

References

1. Bruna PJ, Hirsch G, Peyerimhoff SD, Buenker RJ: *Ab initio* SCF and CI calculations for ground and low-lying valence and Rydberg excited states of HOCl and HClO in linear and bent nuclear conformations. *Can J Chem* 1979, 57(1–2):1839–1851.
2. Balucani N, Beneventi L, Casavecchia P, Volpi GG: Dynamics of the reaction O(¹D) + HCl → ClO + H from crossed-beam experiments. *Chem Phys Lett* 1991, 180(1–2):34–40.
3. Matsumi Y, Tonokura K, Kawasaki M, Tsuji K, Obi K: Dynamics of the reactions of O(¹D) with HCl, DCI, and Cl₂. *J Chem Phys* 1993, 98(10):8330–8336.
4. Matsumi Y, Shamsuddin SM: Vibrational and rotational energy distribution of ClO produced in reactions of O(¹D) atoms with HCl, CCl₄, and chlorofluoromethanes. *J Chem Phys* 1995, 103(11):4490–4495.
5. Hernandez ML, Redondo C, Laganà A, de Aspuru GO, Rosi M, Sgamellotti A: An *ab initio* study of the O(¹D)+HCl reaction. *J Chem Phys* 1996, 105(7):2710–2718.
6. Alvarino JM, Bolloni A, Hernández ML, Laganà A: Dependence of Calculated Product Rotational Polarizations on the Scattering Angle for the O(¹D) + HCl Reaction. *J Phys Chem A* 1998, 102(50):10199–10203.
7. Skokov S, Peterson KA, Bowman JM: An accurate *ab initio* HOCl potential energy surface, vibrational and rotational calculations, and comparison with experiment. *J Chem Phys* 1998, 109(7):2662–2671.

8. Alvariño JM, Rodríguez A, Laganà A, Hernández ML: Double-well structure and microscopic branching in the O(¹D) + HCl reaction. *Chem Phys Lett* 1999, **313**(1–2):299–306.
9. Christoffel KM, Kim Y, Skokov S, Bowman JM, Gray SK: Quantum and quasiclassical reactive scattering of O(¹D)+HCl using an ab initio potential. *Chem Phys Lett* 1999, **315**(3–4):275–281.
10. Peterson KA, Skokov S, Bowman JM: A theoretical study of the vibrational energy spectrum of the HOCl/HClO system on an accurate *ab initio* potential energy surface. *J Chem Phys* 1999, **111**(16):7446–7456.
11. Bittererová M, Bowman JM: A wave-packet calculation of the effect of reactant rotation and alignment on product branching in the O(¹D) + HCl → ClO + H, OH + Cl reactions. *J Chem Phys* 2000, **113**(1):1–3.
12. Bittererová M, Bowman JM, Peterson K: Quantum scattering calculations of the O(¹D) + HCl reaction using a new *ab initio* potential and extensions of J-shifting. *J Chem Phys* 2000, **113**(15):6186–6196.
13. Lin SY, Han KL, Zhang JZH: Time-dependent wavepacket study for O(¹D) + HCl ($v^0 = 0, j^0 = 0$) reaction. *Phys Chem Chem Phys* 2000, **2**(11):2529–2534.
14. Martínez T, Hernández ML, Alvariño JM, Laganà A, Aoiz FJ, Menéndez M, Verdasco E: Quasiclassical trajectory simulation of the O(¹D)+HCl → OH+Cl, ClO+H reactions on an improved potential energy surface. *Phys Chem Chem Phys* 2000, **2**(4):589–597.
15. Piermarini V, Balint-Kurti GG, Gray SK, Görgas F, Laganà A, Hernández ML: Wave packet calculation of cross sections, product state distributions, and branching ratios for the O(¹D) + HCl reaction. *J Phys Chem A* 2001, **105**(24):5743–5750.
16. Piermarini V, Laganà A, Balint-Kurti GG: State and orientation selected reactivity of O(¹D) + HCl from wavepacket calculations. *Phys Chem Chem Phys* 2001, **3**(20):4515–4521.
17. Christoffel KM, Bowman JM: A quasiclassical trajectory study of O(¹D) + HCl reactive scattering on an improved *ab initio* surface. *J Chem Phys* 2002, **116**(12):4842–4846.
18. Gogtas F, Bulut N, Akpinar S: Quantum mechanical three-dimensional wavepacket study of the O(¹D)+ClH → ClO+H reaction. *J Mol Struct (THEOCHEM)* 2003, **625**(1–3):177–187.
19. Martínez T, Hernández ML, Alvariño JM, Aoiz FJ, Rábano VS: A detailed study of the dynamics of the O(¹D) + HCl → OH + Cl, ClO + H reactions. *J Chem Phys* 2003, **119**(15):7871–7886.
20. Yang H, Han KL, Nanbu S, Nakamura H, Balint-Kurti GG, Zhang H, Smith SC, Hankel M: Quantum dynamical study of the O(¹D)+HCl reaction employing three electronic state potential energy surfaces. *J Chem Phys* 2008, **128**(1):014308 (1–5).
21. Wei Q, Wu VWK: Quasiclassical trajectory calculations of the isotopic effect on cross-sections of reactions O(¹D) + HCl (DCI, TCI). *Mol Phys* 2009, **107**(14):1453–1456.
22. Ge MH, Zheng YJ: Stereo-dynamics study of O + HCl → OH + Cl reaction on the ³A'', ³A' and ¹A' states. *Theor Chem Acc* 2011, **129**(2):173–179.
23. Gimelshein SF, Levin DA, Alexeenko AA: Modeling of chemically reacting flows from a side jet and high altitudes. *J Spacecraft Rockets* 2004, **41**(4):582–591.
24. Binder AJ, Dawes R, Jasper AW, Camden JP: The role of excited electronic states in hypervelocity collisions: enhancement of the O(³P) + HCl → OCI + H reaction channel. *J Phys Chem Lett* 2010, **1**(19):2940–2945.
25. Camden JP, Dawes R, Thompson DL: Application of interpolating moving least squares fitting to hypervelocity collision dynamics: O(³P) + HCl. *J Phys Chem A* 2009, **113**(16):4626–4630.
26. Han KL, He GZ, Lou NQ: Effect of location of energy barrier on the product alignment of reaction A + BC. *J Chem Phys* 1996, **105**(19):8699–8704.
27. Li RJ, Han KL, Li FE, Lu RC, He GZ, Lou NQ: Rotational alignment of product molecules from the reactions Sr + CH₃Br, C₂H₅Br, n-C₃H₇Br, i-C₃H₇Br by means of PLIF. *Chem Phys Lett* 1994, **220**(3–5):281–285.
28. Han KL, He GZ, Lou NQ: Theoretical studies of product alignment of the reactions Na, F with CH₃. *Chin Chem Lett* 1993, **4**(6):517–520.
29. Wu VWK: Product rotational angular momentum polarization in the H + FCI ($v = 0–5, j = 0, 3, 6, 9$) → HF + Cl. *Phys Chem Chem Phys* 2011, **13**(20):9407–9417.
30. Aoiz FJ, Bañares L, Herrero VJ: Recent results from quasiclassical trajectory computations of elementary chemical reactions. *J Chem Soc, Faraday Trans* 1998, **94**(17):2483–2500.
31. Aldeguende J, de Miranda MP, Haigh JM, Kendrick BK, Sáez-Rábano V, Aoiz FJ: How reactants polarization can be used to change and unravel chemical reactivity. *J Phys Chem A* 2005, **109**(28):6200–6217.

doi:10.1186/1752-153X-7-177

Cite this article as: Ge et al.: The dynamical study of O(¹D) + HCl($v = 0, j = 0$) reaction at hyperthermal collision energies. *Chemistry Central Journal* 2013 **7**:177.

Publish with ChemistryCentral and every scientist can read your work free of charge

"Open access provides opportunities to our colleagues in other parts of the globe, by allowing anyone to view the content free of charge."

W. Jeffery Hurst, The Hershey Company.

- available free of charge to the entire scientific community
- peer reviewed and published immediately upon acceptance
- cited in PubMed and archived on PubMed Central
- yours — you keep the copyright

Submit your manuscript here:
<http://www.chemistrycentral.com/manuscript/>

